Stability of a boron-doped diamond electrode in molten chloride systems

Yuya Kado*, Takuya Goto, Rika Hagiwara

Department of Fundamental Energy Science, Graduate School of Energy Science,

Kyoto University, Yoshida-honmachi, Sakyo-ku, Kyoto 606-8501, Japan

*Phone : +81-75-753-4848   Fax : +81-75-753-5906

Email : yuuya-kado@t02.mbox.media.kyoto-u.ac.jp

Abstract

Stability of a boron-doped diamond as an oxygen evolution electrode material was evaluated at 773 K in molten LiCl-KCl (58.5:41.5 mol%), LiCl-KCl (75:25 mol%), LiCl-CaCl$_2$ (64:36 mol%), LiCl-NaCl-CaCl$_2$ (52.3:13.5:34.2 mol%). In molten LiCl-KCl systems, the BDD is stable at 773K regardless of the concentration of oxide ion and the composition of the melt. In molten LiCl-CaCl$_2$ and LiCl-NaCl-CaCl$_2$, the BDD electrode is less stable than in molten LiCl-KCl systems.

Keywords: inert anode; boron-doped diamond electrode; oxygen evolution; molten alkali chlorides

2

1. Introduction

Molten alkali chlorides are attractive electrolytes having a lot of excellent features such as thermal and/or chemical stability, wide electrochemical windows, high conductivity and high solubility of other substances. This is why electrochemical processes with molten alkali chlorides are used for the production of alkali, alkaline earth and rare earth metals which are impossible or difficult to obtain by electrochemical processes in aqueous solutions [1].

In recent years, new reduction processes of metal oxides with molten chlorides are proposed to obtain those metals [2-5]. In these reduction processes, oxide ion is generated as a by-product in the electrolytes and smooth removal of it is essential for the improvement of the processes. Carbon has been used for a consumable anode in order to remove oxide ion in the electrolytes, however, the use of carbon anodes in the electrochemical reduction of metal oxides in high-temperature molten salts evolves carbon monoxide and/or dioxide leading to the dispersion of carbon particles into the melts. In our previous studies, a boron-doped diamond (BDD) electrode was found to act as an oxygen evolution electrode in molten LiCl-KCl-Li_2O system at 723 K [6] and molten LiCl-NaCl-$CaCl_2$-Li_2O system at 773 K [7]. On the other hand, the thermal

degradation of diamond has been reported and its decomposition temperature has been

considered to depend significantly on the crystallinity, plane direction and amount of

doped boron [8-11]. Therefore it is required to investigate the thermal stability of the

BDD electrode employed in this study.

In addition, high solubilities of oxides in the electrolytes are also important for

efficient electrochemical reduction of metal oxides. The solubilities of oxides have been

measured in various molten chlorides for the survey of the system which can dissolve a

large amount of oxides [7,12]. It has been found that the solubility significantly depends

on the composition of the melts.

In the present study, thermal stability of the BDD electrode was investigated in

oxygen atmosphere by thermogravimetry and its electrochemical stability was evaluated

in eutectic LiCl:KCl (58.5:41.5 mol%), LiCl-KCl (75:25 mol%), eutectic LiCl-CaCl$_2$

(64:36 mol%), eutectic LiCl-NaCl-CaCl$_2$ (52.3:13.5:34.2 mol%) at 773 K. The eutectic

compositions were selected based on the reported phase diagrams [13-15].

2. Experimental

A boron-doped diamond (BDD) electrode (Diahem^R, Permelec Electrode Ltd.,

thickness: 2-3 μm, substrate: Si) was used as a working electrode. An aluminum plate

(Nilaco Corp., 99.2 %) was employed for a counter electrode. The Ag^+/Ag reference

electrode was prepared by immersing a silver wire (Japan Metal Service, 99.99 %) in

each melt containing 0.5 mol% AgCl (Wako Pure Chemical Co. Ltd., 99.5 %) in a Pyrex

glass tube with the thin bottom. The potential of the reference electrode was

standardized against the Cl_2/Cl^- redox couple.

Reagent-grade LiCl (Aldrich-APL 99.99 %), KCl (Aldrich-APL 99.99 %),

NaCl (Aldrich-APL 99.99 %) and $CaCl_2$ (Aldrich-APL 99.98 %) were used for the melt

after vacuum drying at 573 K for 24 hours. Li_2O (Aldrich. 97 %) was used as an oxide

ion source which was directly added into the melt after vacuum drying at 453 K for 24

hours. All the experiments were conducted in a glove box filled with argon with a

gas-refining instrument (MIWA, MS3-H60SN) under dried and deoxygenated

atmosphere. The concentration of water and oxygen gas in the atmosphere were always

monitored and kept less than 1 ppm.

Determination of the thermal decomposition temperature of a BDD electrode

was performed by a differential thermogravimetric analyzer (Shimadzu Co., Ltd.,

DTG-60/60H). After the dissolution of the silicon substrate, thermal analysis was

performed under the flow oxygen gas (30 ml min^{-1}). Platinum cell was used and the

temperature was changed from the room temperature to 1273 K. The heating rate was 1 K min^{-1}. Electrochemical measurements were performed using an electrochemical measurement system (Hokuto Denko Corp., HZ-3000). The sampled gases during and after electrolysis were analyzed by an oxygen gasometer (Panametric Japan Co. Ltd., OX-2) and infrared spectrometer (BIORAD Ltd., FTS-155). The BDD electrode before and after the electrolysis was analyzed by scanning electron microscopy (Hitachi, Ltd., S-2600H), X-ray diffraction (Rigaku, MultiFlex), and Micro-Raman spectroscopy (Jobin-Yvon, Labram spectrometer).

3 . Results and discussion

3.1 Thermal stability of a boron-doped diamond

A BDD electrode was crushed and the fragments were immersed in aqueous potassium hydroxide (> 50 wt%) at 60 ° C for a week to eliminate the silicon substrate. Elemental silicon dissolves in dense alkaline aqueous solution according to the following reaction (1).

$$Si + 2OH^- + H_2O \rightarrow SiO_3^{2-} + 2H_2\uparrow \qquad (1)$$

6
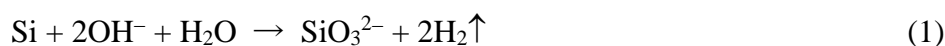
The result of thermogravimetric analysis of the recovered BDD is shown in Fig.1. The

weight loss was observed at 870 to 1100 K, indicating that the BDD electrode is at least

thermally stable and has a possibility to be used as an oxygen evolution electrode at

lower than 870 K. The sample of about 0.9 mg remained at higher than 1200 K is

attributed to residual silicon and/or silicon dioxide. After the measurement, no traces of

BDD were observed in the cell. Diamond is considered to react with O_2 gas to form CO

and/or CO_2 according to the reactions (2) and (3).

$$C + \frac{1}{2}O_2 \rightarrow CO \tag{2}$$

$$C + O_2 \rightarrow CO_2 \tag{3}$$

3.2 Oxygen gas evolution on the BDD electrode in molten chlorides

Figure 2 shows cyclic voltammograms of the BDD electrode after the addition

of Li_2O into eutectic LiCl-KCl (58.5:41.5), LiCl-KCl (75:25), eutectic LiCl-CaCl$_2$ and

eutectic LiCl-NaCl-CaCl$_2$ at 773 K. Anodic currents are observed at around -1.2 V vs.

Cl$_2$/Cl$^-$ in eutectic LiCl-KCl (58.5:41.5), LiCl-KCl (75:25) and -0.7 V vs. Cl$_2$/Cl$^-$ in

molten LiCl-CaCl$_2$ and LiCl-NaCl-CaCl$_2$. In order to investigate the reaction, the gases

generated during potentiostatic electrolysis were analyzed. Figure 3 shows the variation

of the concentration of oxygen gas during the potentiostatic electrolysis at -0.8 V vs.

Cl_2/Cl^- in eutectic LiCl-KCl. It increased as the passage of time. No other gaseous

species such as CO and CO_2 were not detected by infrared spectroscopy as shown in Fig.

4, where IR spectra for CO and CO_2 were also drawn as references. Supposing all the

currents are due to oxygen gas evolution, the current efficiency is calculated to be

almost 100% from the deviation of pressure during the electrolysis in an evacuated cell.

In addition, no weight loss of the BDD electrode was observed. Thus these currents are

attributed to the oxidation of oxide ion to form oxygen gas, which are similar to the

results in our previous study [6,7].

$$O^{2-} \rightarrow \frac{1}{2}O_2 \uparrow + 2e^- \tag{4}$$

Here, the potentials for the oxygen gas evolution are more positive by 0.5 V in

LiCl-CaCl$_2$ and LiCl-NaCl-CaCl$_2$ than that in LiCl-KCl systems. This result suggests

that the coordinating environment of oxide ion in the melts is different among them.

Conceivable reason is the difference of the interaction between oxide ion and its

coordinating cations. The interaction of O^{2-} ion with dipositive Ca^{2+} ion is considered to

be stronger than that with Li^+ and K^+ ions. The stabilities of solid oxides improve in the

following order: $K_2O < Li_2O < CaO$ [16,17] and this tendency corresponds to the

obtained result in the present study.

8

In addition, the standard potential of O_2/O^{2-} against Cl_2/Cl^-, $E^0_{O_2/O^{2-}}$ (vs. Cl_2/Cl^-),

in $LiCl$-Li_2O and $CaCl_2$-CaO systems is calculated based on thermodynamic data. The

standard potential is given by the following equation:

$$E^0_{O_2/O^{2-}} \text{(vs. } Cl_2/Cl^-) = E^0_{M^{n+}/M} \text{(vs. } Cl_2/Cl^-) - E^0_{M^{n+}/M} \text{(vs. } O_2/O^{2-}) \tag{5}$$

where $E^0_{M^{n+}/M}$ (vs. O_2/O^{2-}) is the standard potential of M^{n+}/M (M = Li, Ca) against

O_2/O^{2-} and $E^0_{M^{n+}/M}$ (vs. Cl_2/Cl^-) is that against Cl_2/Cl^-. These standard potentials are also
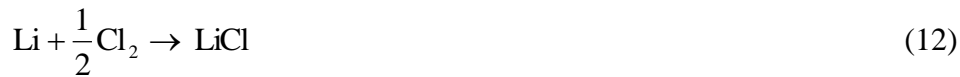
expressed as follows.

$$E^0_{Li^+/Li} \text{(vs. } O_2/O^{2-}) = \frac{\Delta G^0_f(Li_2O)}{2F} \tag{6}$$

$$E^0_{Ca^{2+}/Ca} \text{(vs. } O_2/O^{2-}) = \frac{\Delta G^0_f(CaO)}{2F} \tag{7}$$

$$E^0_{Li^+/Li} \text{(vs. } Cl_2/Cl^-) = \frac{\Delta G^0_f(LiCl)}{F} \tag{8}$$

$$E^0_{Ca^{2+}/Ca} \text{(vs. } Cl_2/Cl^-) = \frac{\Delta G^0_f(CaCl_2)}{2F} \tag{9}$$

Here, $\Delta G^0_f(Li_2O)$, $\Delta G^0_f(CaO)$, $\Delta G^0_f(LiCl)$ and $\Delta G^0_f(CaCl_2)$ are the standard free

energy of formation of pure chemicals at 773 K [16,17].

$$2Li + \frac{1}{2}O_2 \rightarrow Li_2O \tag{10}$$

$$Ca + \frac{1}{2}O_2 \rightarrow CaO \tag{11}$$

$$Li + \frac{1}{2}Cl_2 \rightarrow LiCl \tag{12}$$

$$Ca + Cl_2 \rightarrow CaCl_2 \tag{13}$$

The calculated values are summarized in Table 1. The difference of $E^0_{O_2/O^{2-}}$ (vs. Cl_2/Cl^-)

obtained from eqs. 5-9 is 0.358 V ascribed to the difference of the melts, LiCl-KCl

mixtures and the melts containing $CaCl_2$, and this value is smaller than that obtained

from the observed potentials. It suggests that the overpotential for oxygen gas evolution

in $LiCl$-$CaCl_2$ and $LiCl$-$NaCl$-$CaCl_2$ is higher than that in LiCl-KCl mixtures. A large

overpotential might be due to strong adsorption of generated oxygen gas, which is

caused by the low wettability of the melts containing $CaCl_2$ [7].

3.3 Electrochemical stability of the BDD electrode in a LiCl-KCl eutectic melt

Galvanostatic electrolysis at 12 mA cm^{-2} for 20 h was conducted in order to

investigate the electrochemical stability of the BDD electrode in LiCl-KCl eutectic

melts containing 1.0 and 2.0 mol% of Li_2O at 773 K. The quantity of electricity was 800

C cm^{-2}. The potential of the BDD electrode was kept roughly around -1.0 V (vs.

Cl_2/Cl^-) during the galvanostatic electrolysis accompanied by oxygen evolution.

Oxygen gas evolution was considered to continuously occur during the electrolysis

since CO and CO_2 were not observed by IR spectroscopy in the gaseous sample from

the electrolysis cell. Figure 5 shows SEM images of the BDD electrode before and after

the galvanostatic electrolysis at 773 K, where the morphologies are almost identical.

10

XRD patterns and micro-Raman spectra of the electrode before and after electrolysis also reveal that the diamond structure is preserved after the electrolysis as shown in Figs. 6 and 7. In addition, these results suggest that the stability of the BDD electrode does not depend on O^{2-} concentration in the melt. However, apparent consumption of the electrode was observed after electrolysis at temperatures higher than 823 K. Thus the BDD electrode is concluded to be electrochemically stable and act as an oxygen evolution electrode at temperatures lower than 773 K in molten $LiCl$-KCl-Li_2O systems. The difference of the decomposition temperatures between the electrochemical oxidation in this section and the chemical oxidation in section 3.1 can be ascribed to the difference of activity of oxygen gas adsorbed on the electrode surface. It is considered that oxygen gas generated by electrolysis on the BDD electrode is adsorbed on the electrode surface and its high activity leads to chemical consumption of the BDD electrode at lower temperatures.

3.4 Dependence of the stability on the melt composition

The stability of the BDD electrode as an oxygen evolution electrode in molten $LiCl$-KCl (75:25), eutectic $LiCl$-$CaCl_2$ and eutectic $LiCl$-$NaCl$-$CaCl_2$ was examined in

11

the same manner as described for a LiCl-KCl eutectic melt. The potentials during the galvanostatic electrolysis were around -1.0 V (vs. Cl_2/Cl^-) in LiCl-KCl (75:25), -0.05 V (vs. Cl_2/Cl^-) in eutectic LiCl-CaCl$_2$ and eutectic LiCl-NaCl-CaCl$_2$. Figure 6 shows the SEM images before and after galvanostatic electrolysis at 12 mA cm^{-2} for 20 h in eutectic LiCl:KCl (58.5:41.5) (a), LiCl-KCl (75:25) (b), eutectic LiCl-CaCl$_2$ (c) and eutectic LiCl-NaCl-CaCl$_2$ (d) containing 1.0 mol% Li$_2$O. The BDD electrode is as stable in LiCl-KCl (75:25) as in eutectic LiCl-KCl (58.5:41.5). This result suggests that the stability of the BDD electrode is not dependent on the melt composition in molten LiCl-KCl systems and the BDD electrode is considered to act as an oxygen evolution electrode in any compositions of LiCl-KCl at 773 K.

In molten LiCl-CaCl$_2$ and LiCl-NaCl-CaCl$_2$, although no notable change was observed by XRD and Raman spectroscopy, SEM images in Fig.6 apparently show the BDD electrode is less stable as an oxygen evolution electrode than in LiCl-KCl systems. However, the anodic currents attributed to CO and/or CO$_2$ evolution are not observed in Fig.2. Conceivable explanation is chemical consumption of the BDD electrode by oxygen gas electrochemically generated on the electrode. This result might be attributed to the low wettability of the melts containing CaCl$_2$, leading stronger adsorption of oxygen gas on the electrode surface and higher overpotential for oxygen gas evolution.

12

Therefore high activity of oxygen gas is considered to chemically facilitate the consumption of the BDD electrode. Another conceivable reason is the catalytic effect of calcium in the electrolyte. It is possible that calcium deposited at the cathode diffuses into the electrolyte and chemically interacts with carbon atom of the diamond surface.

4. Conclusion

The stability of a boron-doped diamond electrode as an oxygen evolution electrode was evaluated in molten LiCl:KCl (58.5:41.5), LiCl-KCl (75:25), LiCl-CaCl$_2$ (64:36), LiCl-NaCl-CaCl$_2$ (52.3:13.5:34.2) at 773 K. In molten LiCl-KCl systems, the BDD electrode is stable and its stability does not depend on the concentration of oxide ion and the melt composition. Thus the BDD electrode has a potential to be employed for the inert anode in molten LiCl-KCl with any compositions at 773 K. In molten LiCl-CaCl$_2$ and LiCl-NaCl-CaCl$_2$, however, the BDD electrode is less stable than in molten LiCl-KCl systems, which is conceivably due to the low wettability of the melts containing CaCl$_2$. As a result in the present study, it is suggested that molten LiCl-KCl (75:25) is one of the best candidate electrolytes for the reduction processes of metal oxides when combined with the BDD counter electrode taking account of the factors

13

such as high stability of the electrode and the large solubility of oxides at relatively low

temperatures.

References

[1] D. J. Fray, in: Proc. 7th Int. Conf. on Molten Slags, Fluxes and Salts, South African Institute of Mining and Metallurgy, Cape Town, 2004, p.7.

[2] G. Z. Chen, D. J. Flay, T. W. Farthing, Nature 407 (2000) 361.

[3] Y. Sakamura, M. Kurata and T. Inoue, J. Electrochem. Soc., 153 (2006) D31.

[4] R. O. Suzuki and K. Ono, in: Proc. 13th Int. Symp. on Molten Salt, 2002, Electrochemical Society, Pennington, 2002, p. 810.

[5] T. Usami, M. Kurata, T. Inoue, H. E. Sims, S. A. Beetham, and J. A. Jenkins, J.Nucl. Mater., 300 (2002) 15.

[6] T. Goto, Y. Araki and R. Hagiwara, Electrochem. Solid-State Lett., 9 (2006) D5.

[7] Y. Kado, T. Goto and R. Hagiwara, J. Electrochem. Soc., 155 (2008) E85.

[8] Q. Sun and M. Alam, J. Electrochem. Soc., 139 (1992) 933.

[9] M. Alam and Q. Sun, J. Mater. Sci. Lett., 12 (1993) 1389.

[10] P. John, N. Polwart, C.E. Troupe and J.I.B. Wilsonb, Diamond Relat. Mater., 11 (2002) 861.

[11] H.S. Li, Y.X. Qi, J.H. Gong, M. Wang and M.S. Li, *Int.* J. Refract. Met. Hard Mater., In Press, Corrected Proof, Available online 22 August 2008.

[12] Y. Kado, T. Goto and R. Hagiwara, J. Chem. Eng. Data, 53 (2008) 2816.

[13] E. Elchardus and P. Laffitte, Bull. Chim., France, 51 (1932) 1572.

[14] K.H. Mahendran, S. Nagaraj, R. Sridharan, T. Gnanasekaran, J. Alloy. Comp. 325 (2001) 78.

[15] G. A. Bukhalove and A. S. Arabadzhen, Zh. Neorgan. Khim., 7 (1962) 2230.

[16] Landolt-Börnstein, SGTE, Springer-Verlag, Berlin-Heidelberg (1999).

[17] Landolt-Börnstein, SGTE, Springer-Verlag, Berlin-Heidelberg (2001).

List of figure and table captions

Table 1 The calculed values of the stanrad formal potentials at 773 K (M = Li in LiCl, Ca in $CaCl_2$)

Fig. 1 The TGA data of BDD in oxygen atmosphere (Heating rate : 1 K min^{-1}).

Fig.2 Cyclic voltammograms on the BDD electrode in molten chlorides containing 1.0 mol% Li_2O at 773 K. Scan rate is 0.1 V s^{-1}. [(a) eutectic LiCl-KCl, (b) LiCl-KCl (75 : 25 mol%), (c) eutectic $LiCl-CaCl_2$, (d) eutectic $LiCl-NaCl-CaCl_2$].

Fig.3 The variation of the concentration of oxygen gas during the potentiostatic electrolysis at − 0.8 V vs. Cl_2/Cl^- in eutectic LiCl-KCl containing 2.0 mol% Li_2O at 773 K.

Fig.4 Infrared spectra of the gas sampled after the potentiostatic electrolysis at − 0.8 V vs. Cl_2/Cl^- in eutectic LiCl-KCl containing 2.0 mol% Li_2O at 773 K.

Fig.5 SEM images of the BDD electrode before and after galvanostatic electrolysis in a LiCl-KCl eutectic melt containing Li_2O [(a) as-received, (b) 1.0 mol% Li_2O, (c) 2.0 mol% Li_2O].

Fig.6 XRD patterns of the BDD electrode before and after the galvanostatic electrolysis in a LiCl-KCl eutectic melt containing Li_2O at 773 K [(a) as-received, (b) 1.0 mol%

Li_2O, (c) 2.0 mol% Li_2O].

Fig.7 Raman spectra of the BDD electrode before and after electrolysis in a LiCl-KCl eutectic melt containing Li_2O at 773 K [(a) as-received, (b) 1.0 mol% Li_2O, (c) 2.0 mol% Li_2O].

Fig.8 SEM images of the BDD electrodes before and after galvanostatic electrolysis in molten LiCl-KCl systems containing 1.0 mol% Li_2O [(a) eutectic LiCl-KCl, (b) LiCl-KCl (75:25 mol%), (c) eutectic $LiCl-CaCl_2$, (d) eutectic $LiCl-NaCl-CaCl_2$].
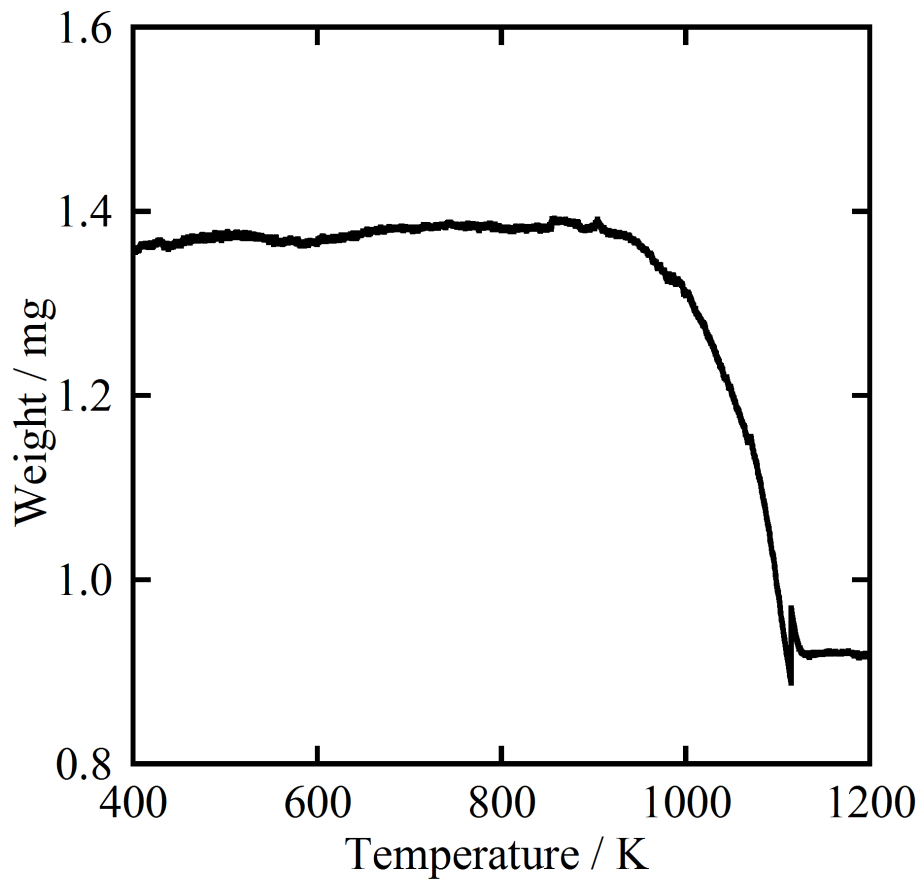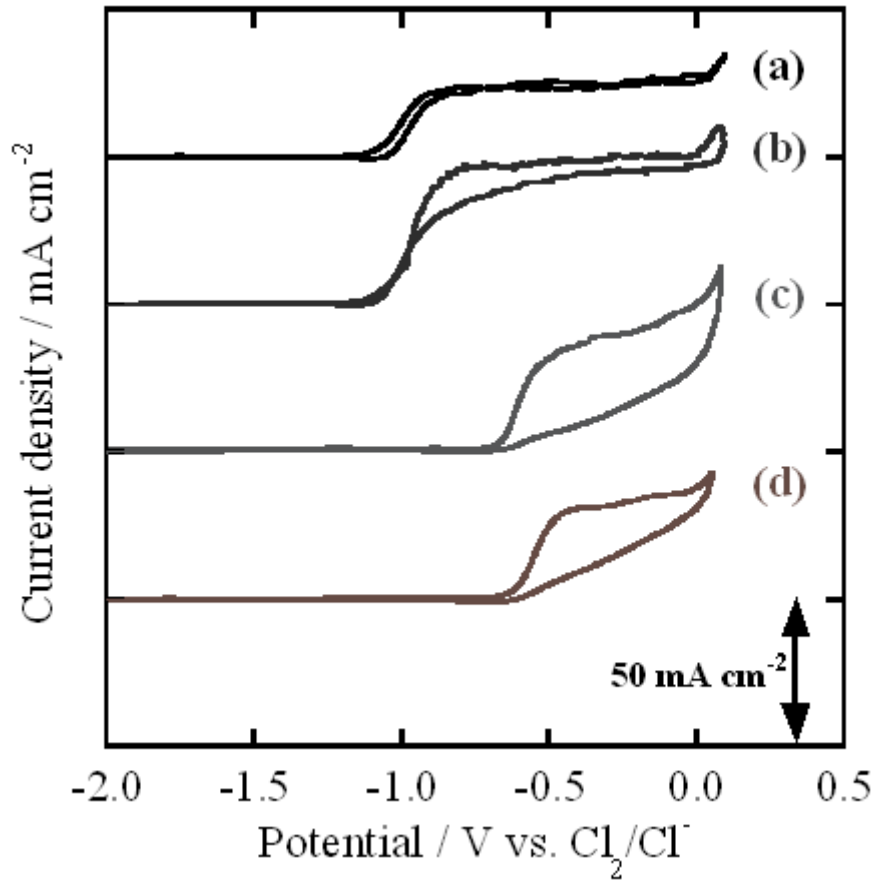
Fig. エラー! メイン文書しかありません。 The TGA data of BDD in oxygen

atmosphere (Heating rate : 1 K min^{-1}).

Fig. 2 Cyclic voltammograms on the BDD electrode in molten chlorides containing 1.0 mol% Li_2O at 773 K. Scan rate is 0.1 V s^{-1}. [(a) eutectic LiCl-KCl, (b) LiCl-KCl (75 : 25 mol%), (c) eutectic LiCl-CaCl$_2$, (d) eutectic LiCl-NaCl-CaCl$_2$].
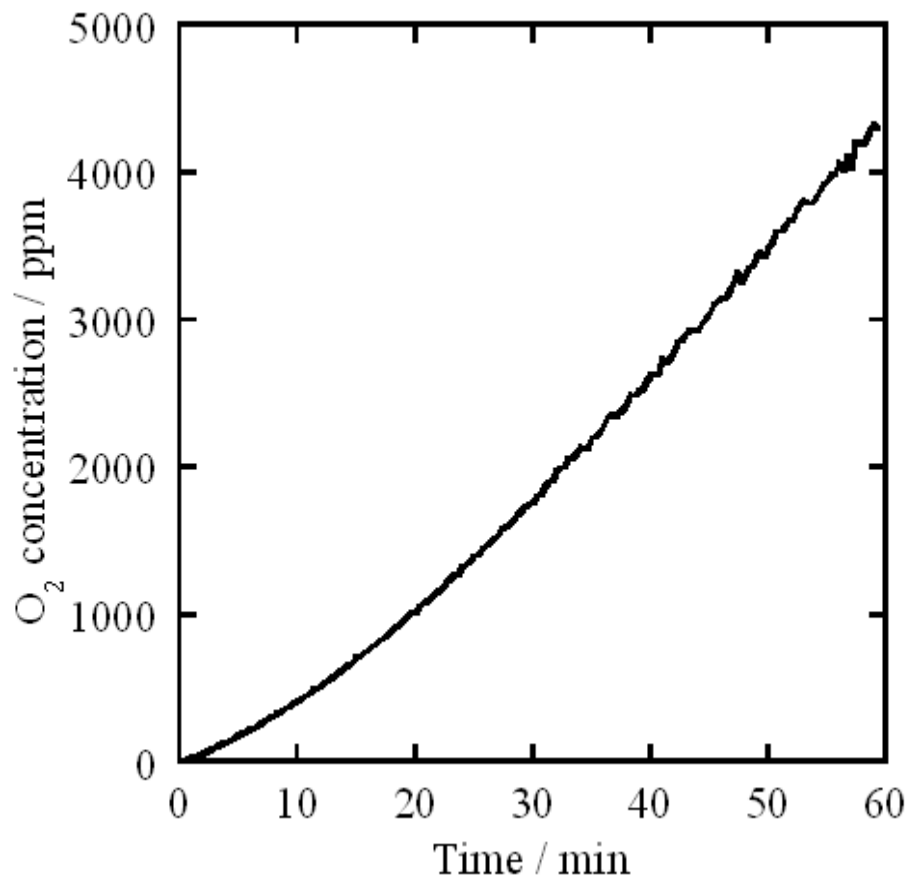
20

Fig.3 The variation of the concentration of oxygen gas during the potentiostatic electrolysis at -0.8 V vs. Cl_2/Cl^- in eutectic LiCl-KCl containing 2.0 mol% Li_2O at 773 K.

Fig.4 Infrared spectra of the gas sampled after the potentiostatic electrolysis at -0.8 V

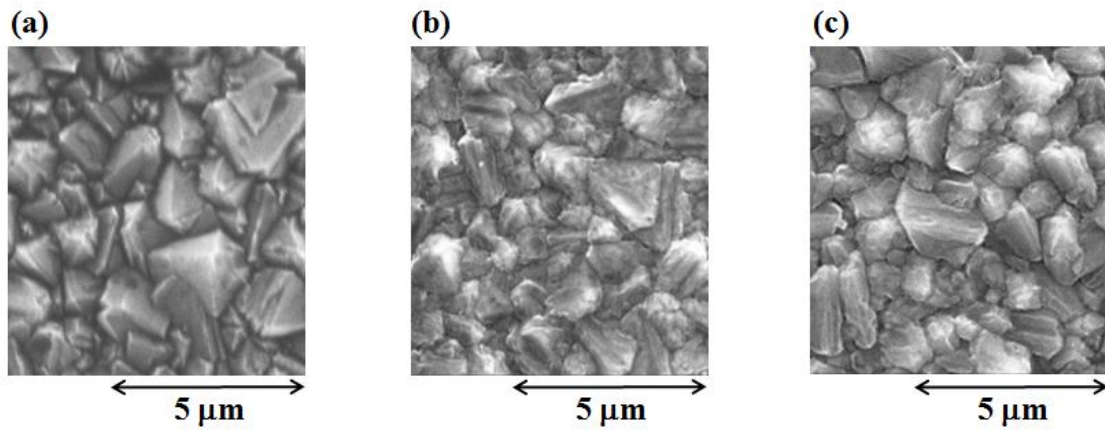vs. Cl_2/Cl^- in eutectic LiCl-KCl containing 2.0 mol% Li_2O at 773 K.

Fig. 5 SEM images of the BDD electrode before and after galvanostatic electrolysis in a LiCl-KCl eutectic melt containing Li_2O [(a) as-received, (b) 1.0 mol% Li_2O, (c) 2.0 mol% Li_2O].
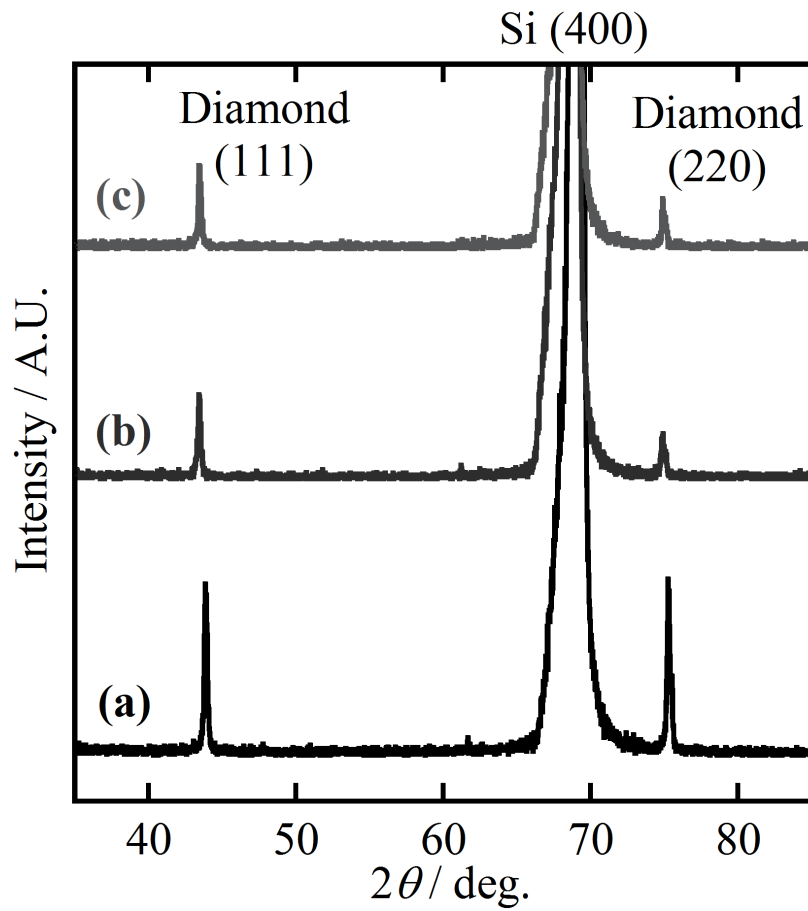
Fig.6 XRD patterns of the BDD electrode before and after the galvanostatic electrolysis in a LiCl-KCl eutectic melt containing Li_2O at 773 K [(a) as-received, (b) 1.0 mol% Li_2O, (c) 2.0 mol% Li_2O].
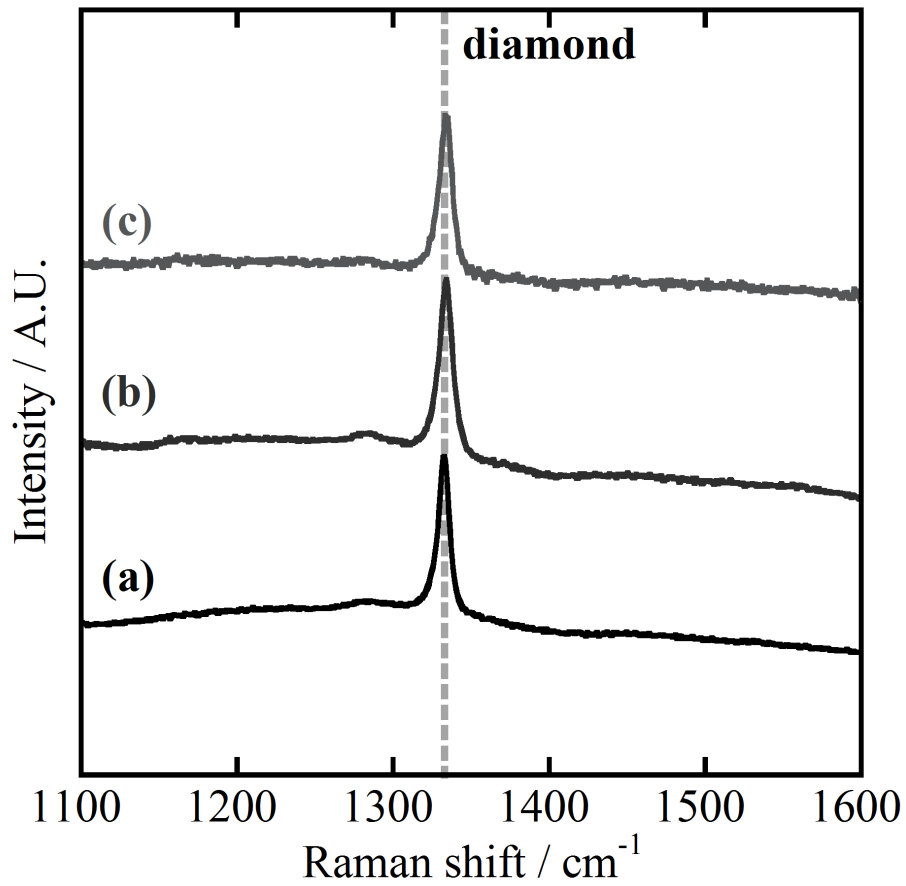
Fig.7 Raman spectra of the BDD electrode before and after electrolysis in a LiCl-KCl eutectic melt containing Li_2O at 773 K [(a) as-received, (b) 1.0 mol% Li_2O, (c) 2.0 mol% Li_2O].
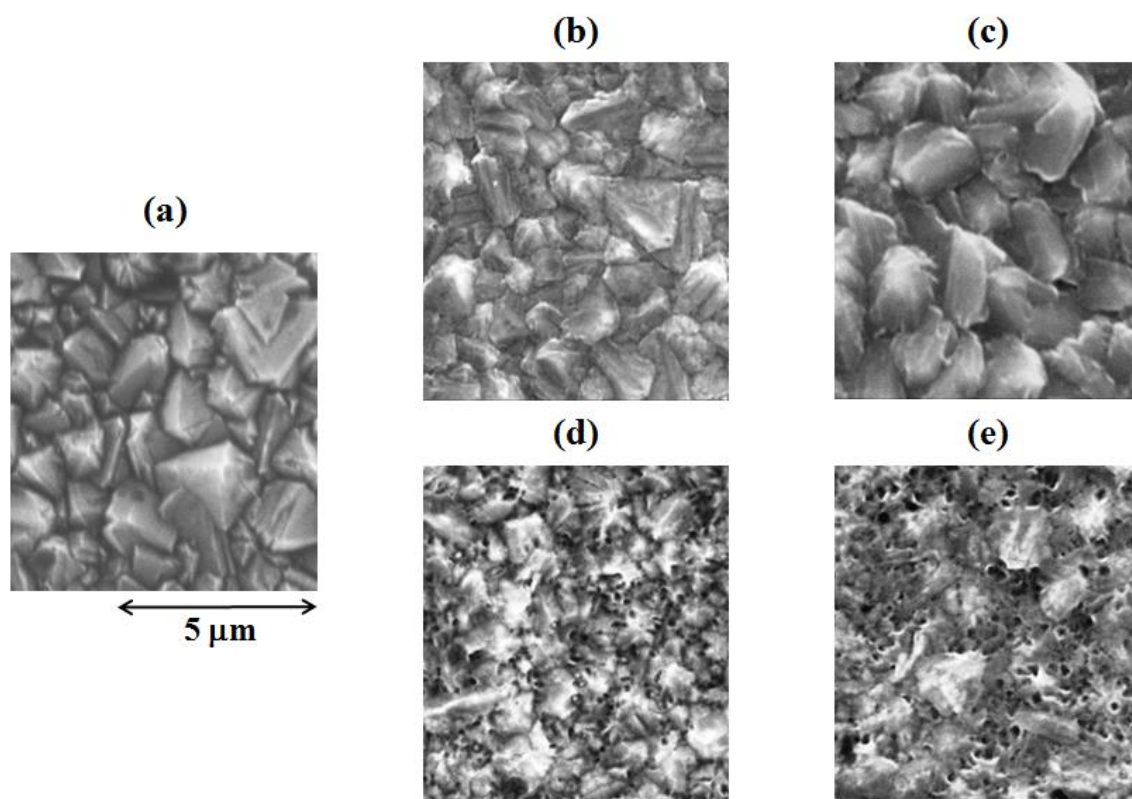
Fig. 8 SEM images of the BDD electrodes before and after galvanostatic electrolysis in molten LiCl-KCl systems containing 1.0 mol% Li_2O [(a) eutectic LiCl-KCl, (b) LiCl-KCl (75:25 mol%), (c) eutectic $LiCl-CaCl_2$, (d) eutectic $LiCl-NaCl-CaCl_2$].

Table 1 The calculed values of the stanrad formal potentials at 773 K (M = Li in LiCl,

Ca in CaCl$_2$)

Melt	$E^0_{M^{n+}/M}$ / V vs. O$_2$/O^{2-}	$E^0_{M^{n+}/M}$ / V vs. Cl$_2$/Cl$^-$	$E^0_{O_2/O^{2-}}$ / V vs. Cl$_2$/Cl$^-$
LiCl	− 2.5742	− 3.5741	− 0.9999
CaCl$_2$	− 2.8705	− 3.5127	− 0.6422